UC Davis

UC Davis Previously Published Works

Title

Regulatory mechanisms of miR-96 and miR-184 abnormal expressions on otic vesicle development of zebrafish following exposure to β-diketone antibiotics

Permalink

https://escholarship.org/uc/item/2459956g

Authors

Li, Jieyi
Ling, Yuhang
Huang, Wenhao
et al.

Publication Date

2019

DOI

10.1016/j.chemosphere.2018.09.118

Peer reviewed

eScholarship.org Powered by the California Digital Library
University of California

Chemosphere 214 (2019) 228–238

Contents lists available at ScienceDirect

Chemosphere

journal homepage: www.elsevier.com/locate/chemosphere

Regulatory mechanisms of miR-96 and miR-184 abnormal expressions on otic vesicle development of zebrafish following exposure to β-diketone antibiotics

Jieyi Li [a, b], Yuhang Ling [a], Wenhao Huang [a], Limei Sun [a], Yanyan Li [a], Caihong Wang [a], Yuhuan Zhang [a], Xuedong Wang [c, **], Randy A. Dahlgren [d], Huili Wang [a, *]

[a] Zhejiang Provincial Key Laboratory of Medical Genetics, Key Laboratory of Laboratory Medicine, Ministry of Education, School of Laboratory Medicine and Life Sciences, Wenzhou Medical University, Wenzhou, 325035, Zhejiang, China
[b] Beijing Key Laboratory of Cardiometabolic Molecular Medicine, State Key Laboratory of Natural and Biomimetic Drugs, Institute of Molecular Medicine, Peking University, Beijing, 100871, China
[c] National and Local Joint Engineering Laboratory of Municipal Sewage Resource Utilization Technology, School of Environmental Science and Engineering, Suzhou University of Science and Technology, Suzhou, 215009, China
[d] Department of Land, Air and Water Resources, University of California-Davis, CA, 95616, USA

HIGHLIGHTS

- miR-96 and -184 down-regulation following DKA exposure during embryonic development.
- miR-96 play a critical role in otic vesicle development and formation of hearing.
- miR-96 influences otic vesicle development by affecting hair cell differentiation.
- miR-184 is involved in otic vesicle construction during embryonic development.

GRAPHICAL ABSTRACT

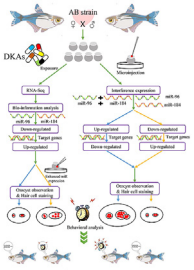

ARTICLE INFO

Article history:
Received 16 August 2018
Received in revised form
17 September 2018
Accepted 18 September 2018
Available online 19 September 2018

Handling Editor: David Volz

Keywords:
β-Diketone antibiotics
Hearing loss
miR-96
miR-184
Ototoxicity
Otic vesicle

ABSTRACT

Chronic ototoxicity of β-diketone antibiotics (DKAs) to zebrafish (*Danio rerio*) was explored in detail by following abnormal expressions of two hearing-related miRNAs. Dose-dependent down-regulation of miR-96 and miR-184 was observed in otoliths during embryonic-larval development. Continuous DKA exposure to 120-hpf larva decreased sensitivity to acoustic stimulation. Development of otolith was delayed in treatment groups, showing unclear boundaries and vacuolization at 72-hpf, and utricular enlargement as well as decreased saccular volume in 96-hpf or latter larval otoliths. If one miRNA was knocked-down and another over-expressed, only a slight influence on morphological development of the otic vesicle occurred, but knocked-down or over-expressed miRNA both significantly affected zebrafish normal development. Injection of miR-96, miR-184 or both micRNA mimics to yolk sac resulted in marked improvement of otic vesicle phenotype. However, hair cell staining showed that only the injected miR-96 mimic restored hair cell numbers after DKA exposure, demonstrating that miR-96 played an important role in otic vesicle development and formation of hearing, while miR-184 was only involved in otic vesicle construction during embryonic development. These observations advance our understanding

* Corresponding author.
** Corresponding author.
E-mail addresses: zjuwxd@163.com (X. Wang), whuili@163.com (H. Wang).

https://doi.org/10.1016/j.chemosphere.2018.09.118
0045-6535/© 2018 Elsevier Ltd. All rights reserved.

of hearing loss owing to acute antibiotic exposure and provide theoretical guidance for early intervention and gene therapy for drug-induced diseases.

© 2018 Elsevier Ltd. All rights reserved.

1. Introduction

Fluoroquinolones (FQs) and tetracyclines (TCs) are two important classes of pharmaceutical and personal care products designated as β-diketone antibiotics (DKAs) due to the presence of a β-diketone functional group in their molecular structure. DKAs are widely utilized because of their excellent broad-spectrum antibacterial effect (Qu et al., 2010; Yoon et al., 2010). Frequent usage and continuous emission of DKAs into the environment result in DKAs becoming a "pseudo-persistent" pollutant, in spite of their comparatively short half-lives. As a result, DKAs can lead to metabolic and cumulative toxicity, and cause ecosystem pressure on numerous organisms (Brain et al., 2005; Sarmah et al., 2006). Toxicity of FQs and TCs has been widely reported, including a range of cardiovascular diseases and arthropathy (Mulgaonkar et al., 2012). FQs can significantly inhibit the activity of acetylcholinesterase, leading to potential neurotoxicity (Wang et al., 2009). Additionally, TCs cause impaired organ metabolism and fatty liver formation (Yin et al., 2006), and inhibit the activity of superoxide dismutase in liver causing metabolic disturbance in zebrafish embryos (Wang et al., 2014).

In real-world environments, residual components of antibiotics are very complex and may contribute to joint (i.e., interactive) toxicological effects (Ding et al., 2013; Melvin et al., 2014). Our previous research examined the effects of three representative FQs (enrofloxacin, ofloxacin and ciprofloxacin) and three TCs (chlortetracycline, oxytetracycline and doxycycline) on joint toxicity to various tissues and organs including the immune, reproductive and nervous systems in zebrafish (*Danio rerio*) (Li et al., 2016a). Some FQ family members, such as ciprofloxacin (Etminan et al., 2017; Samarei et al., 2014), are reported to cause ototoxic effects, while some TC family members, such as doxycycline (Chotmongkol et al., 2012) and minocycline (Corbacella et al., 2004) function to restore hearing loss. However, there is a paucity of data regarding chronic joint DKA exposure on hearing impairments, especially studies examining the molecular response to DKA exposure.

Li and coworkers reported abnormal expression of a large number of microRNAs (miRNAs) after DKA exposure based on high throughput RNA sequencing (Li et al., 2016b). The miRNAs are an abundant class of non-coding RNAs that can potentially control dozens of genes. Multiple miRNAs have been shown to collaborate in targeting extensive cellular processes and molecular pathways (Vlachos et al., 2015; Wienholds and Plasterk, 2005b). Numerous studies attributed abnormal miRNA expression and regulation to a variety of diseases, such as cancer (Kaur et al., 2016; Zhao et al., 2017), heart disease (Yang et al., 2017) and brain development (Xu et al., 2017). For example, miR-96 was reported as a hearing loss factor (Lewis et al., 2016; Soldà et al., 2012), and miR-184 showed a high correlation with cancer (Zhou et al., 2017) and nervous system development (Liang et al., 2017; McKiernan et al., 2012). Although our previous studies speculated that miR-96 and miR-184 might have some functional relevance (Li et al., 2016b), no direct evidence or additional reports have examined their contributions to molecular mechanisms regulating hearing functions. Thus, additional research is highly warranted from a public health perspective given that some FQs may cause ototoxicity (Etminan et al., 2017; Samarei et al., 2014) while some related TCs function to restore hearing loss (Chotmongkol et al., 2012; Corbacella et al., 2004). Notably, the underlying molecular mechanisms concerning DKA impacts on human hearing loss have yet to be rigorously investigated.

Based on our previous research (Li et al., 2016b), miR-96 and miR-184 were identified as key factors warranting further study to investigate the role of DKAs on hearing functions. Therefore, this research focused on expression changes of miR-96 and miR-184, their target genes and functional relevance in response to DKA exposure of zebrafish embryos. The effects of abnormal expressions of miR-96 and miR-184 on otic vesicle development were investigated in detail using manual intervention of miRNA expression, behavioral analysis, morphological observations and hair cell staining. The findings of this study further our understanding of deafness diseases due to antibiotic exposure, and also provide theoretical guidance for early intervention and gene therapy for drug-induced diseases.

2. Material and methods

2.1. Ethics statement

The Institutional Animal Care and Use Committee (IACUC) at Wenzhou Medical University approved our study plan for ethical use of zebrafish (*Danio rerio*). All studies were carried out in strict accordance to IACUC guidelines. Dissection was performed on ice to minimize suffering.

2.2. Chemical reagents and exposure protocols

Six DKAs were purchased from Amresco (Solon, OH, USA); CAS number, purity, chemical structure and molecular weight are shown in Table S1 and Fig. S1. Wild type adult zebrafish (AB strain) were purchased from a local supplier and adapted to laboratory conditions with a light/dark, 14 h/10 h cycle in a circulation system with dechlorinated tap water (pH 7.0–7.5) at a constant temperature ($27 \pm 0.5\,^{\circ}C$). Zebrafish maintenance followed Westerfield (1995). Embryos were exposed to a series of DKA concentrations (0, 12.5 and 25 mg L^{-1} (25 mg L^{-1} corresponding to 11.5, 12.6, 11.6, 8.1, 8.1 and 9.0 μM for ofloxacin, ciprofloxacin, enrofloxacin, doxycycline, chlortetracycline and oxytetracycline, respectively)). DKA stock solutions were composed of six DKA species with equal weight concentrations and equal volumes of each species. Zebrafish were continuously exposed to DKAs from embryos (2 hpf) to larvae (5 dpf) stage. The DKA stock solution was prepared by dissolving the six DKA species in ultra-pure water using 0.1 M NaOH as cosolvent; stock solutions were replaced daily to maintain a constant concentration.

2.3. Total RNA extraction

The 72- or 120-hpf zebrafish embryos in each treatment group were collected and rinsed using phosphorous buffer solution (PBS, Solarbio, Beijing, China) in an RNase-free 1.5 mL EP tube. Total RNA was isolated according to the protocol reported by Wu and coworkers (Wu et al., 2015).

2.4. Bioinformatics prediction for target genes of miR-96 and miR-184

Three miRNA databases were used to predict target genes of miR-96 and miR-184: TargetScan (http://www.targetscan.org/), MicroCosm (http://www.ebi.ac.uk/enright-srv/microcosm/, miRBase Targets Release Version v5), and miRanda (http://www.microrna.org/). Only those target genes commonly predicted by all three databases were regarded as reliable. For functional annotation of genes targeted by the miRNAs, Kyoto Encyclopedia of Genes and Genomes (KEGG) functional classification (http://www.genome.jp/kegg/) was performed using the web-based tool, Database for Annotation, Visualization and Integrated Discovery (DAVID, http://david.abcc.ncifcrf.gov/) (Huang et al., 2009). Comparison of sequence homology among different species was conducted using the rVista 2.0 database (https://rvista.dcode.org/). DIANA miRPath V3 software (http://snf-515788.vm.okeanos.grnet.gr/) was used to produce heat maps for miR-96 and miR-184.

2.5. qRT-PCR analysis

Forward primers for the miRNAs were synthesized by Sangon Biotechnology Co. (Shanghai, China) and reverse primers were the universal reverse primers provided by GeneCopoeia (Guangzhou, China) with U6 as the endogenous reference (Table S2). For the target genes, the primers (Table S2) were designed and synthesized by Sangon Biotechnology. Quantification of results was performed using the ΔΔCt method as described by Livak and coworkers (Livak et al., 2001).

2.6. Whole-mount in situ hybridization (W-ISH)

As generalized in Table S3, cDNA probes for miR-96 and miR-184 were synthesized by Sangon Biotechnology Company and labeled with digoxigenin (DIG). Target gene primers were designed with NCBI Primer BLAST (https://www.ncbi.nlm.nih.gov/tools/primer-blast/) and cloned by PCR Master (Roche, Basel, Switzerland). Products were ligated and amplified into T3 vector using the pEASY-T3 Cloning Kit (TransScript, Beijing, China). After digestion by endonuclease SpeI or NcoI (NEB), the T7 High Efficiency Transcription Kit (TransScript) or SP6 RNA Polymerase Kit (Takara, Kusatsu, Japan) were used for *in vitro* transcription and the probes were labeled with DIG RNA Labeling Mix (Roche).

Embryos in each treatment group were treated with 0.5% *N*-phenylthiourea (PTU, Aladdin, Shanghai, China) and aliquots containing 15 embryos were collected in 1.5 mL RNase-free EP tubes. Procedures for whole-mount ISH (W-ISH) followed Thisse et al. (2008).

2.7. Microinjection and phenotype observation

Adult zebrafish were mated and spawned for 10–15 min, and the fertilized eggs were quickly collected for microinjection. MicroRNA mimics and inhibitors for miR-96 and miR-184 were synthesized by GenePharma (Shanghai, China) and used as received. Concentrations of mimics or inhibitors were adjusted to 200 ng μL^{-1} and 2 nL of this solution were injected into each egg (Pli-100A, Warner Instruments, Hamden, USA), and equal amount of 0.1% phenolsulfonphthalein (Sigma, St. Louis, USA) solution was injected as the negative control group; any dead embryos were removed every 12 h.

Thirty embryos or larvae from each treatment were randomly selected and anesthetized with 0.03% tricaine methanesulfonate (buffered MS-222, Sigma, St. Louis, USA) for 30 s before observation using an optical microscope (DM2700 M, Leica, Heidelberg, Germany).

2.8. Behavioral assessment

To assess larval response to external acoustic stimuli, 120-hpf larvae in control and treatment groups were transferred to 96-square-well plates and placed into a DanioVision Observation Chamber (Noldus IT, Wageningen, Netherlands). There was one larva for each well and each plate included one control group and two treatment groups (12.5 and 25 mg L^{-1} DKA concentrations) with 32 larvae for each group and three replications for each plate. Therefore, a total of 96 larvae were used as biological replicates for each treatment. After a 20-min adaptation period, a tapping stimulation was initiated with a total of four tapping intensities. Each plate was tested at least three times, and each test interval was 5 min. Video was collected and analyzed with EthoVision XT software (Noldus IT, Wageningen, Netherlands) to compute the mean speed and mean swim distance in the 15 s interval following tapping stimulation.

2.9. AO-EB staining and DASPEI staining

AO (acridine orange)-EB (ethidium bromide) double staining kits (CA1140, Solarbio, Beijing, China) were used for AO-EB staining. For each treatment group, 20 larvae were randomly selected and transferred to 1.5 mL EP tubes followed by washing three times with PBS buffer (Solarbio, Beijing, China). AO buffer and EB buffer were mixed 1:1 in the dark and then diluted ten times with PBS buffer solution. Larvae were transferred to the diluted buffer solution for 20–30 min in the dark and then anesthetized with 0.03% MS-222 (Sigma, St. Louis, USA) for 30 s before observation with a fluorescence microscope (DM2700 M, Leica, Heidelberg, Germany).

For DASPEI staining, 20 larvae were collected and rinsed with PBS buffer before staining with 0.005% DASPEI (2-[4-(dimethylamino)styryl]-1-ethylpyridinium iodide (Sigma, St. Louis, USA) in the dark for 20 min (Owens et al., 2009). Larvae were then anesthetized and observed as previously described for AO-EB staining.

2.10. Statistical analysis

Each DKA-exposure treatment and control group were conducted with biological and technological triplicates, and all data were recorded as mean ± SD (standard deviation, n = 3). Each biological replicate included 20 zebrafish (female:male = 1:1) and thus 60 zebrafish (3 × 20) were used in each group for qRT-PCR, W-ISH and histopathological observations. One-way analysis of variance (ANOVA) was used to assess DKA treatment effects, followed by Dunnett's tests to independently compare DKA-exposure groups with the control group. All statistical analyses were conducted with SPSS 18.0 (SPSS, Chicago, USA) using $p < 0.05$ or $p < 0.01$ significance levels.

3. Results

3.1. Bioinformatics analysis

The main function of miRNAs is regulating the expression of target genes. In this investigation, the TargetScan database was used to predict target genes for miR-96 and miR-184. TargetScan analysis identified 4329 potential target genes for miR-96 and 801 target genes for miR-184. Among these genes, 337 were co-regulated by both miR-96 and miR-184, which accounted for 8% and 42% of total target genes for miR-96 and miR-184, respectively. These results demonstrate the functional relevance between miR-96 and miR-184 (Fig. S2). Additionally, some target genes with

high total context + scores were selected and screened in the KEGG bank indicating enrichment in metabolic pathways, calcium signaling pathway, ErbB signaling pathway, and other neural related signaling pathways (Fig. 1A).

Analysis of sequence homology was conducted by comparison of zebrafish, rats and mice with the human sequence as a reference. The miR-96 has high sequence homology in all four species (Fig. 1B) and miR-184 in rats, mice and humans (Fig. 1C). While sequence information for miR-184 was not available for zebrafish in the rVista 2.0 database (https://rvista.dcode.org/), it was checked in miRBase and compared with humans. This comparison showed that the sequences for miR-96 and miR-184 were highly conserved across vertebrate species, and only dre-miR-184 exhibited one different base (Fig. 1F).

Pathway enrichment analysis was used to assess functional associations of miR-184 and miR-96 in humans (Fig. 1D) and mice (Fig. 1E) using DIANA miRPath V3 software (http://snf-515788.vm.okeanos.grnet.gr/). Some bio-pathways, co-regulated by miR-184 and miR-96, were found in humans, such as ECM-receptor interaction, prostate cancer and adherens junction. In mice, common functions of the two miRNAs were mainly associated with metabolism of xenobiotics by cytochrome P450 and the Wnt signaling pathway. Currently there is a paucity of information regarding the common functions of miR-96 and miR-184 in zebrafish, which is the focus of this research.

3.2. Expression of miR-96 and miR-184 by W-ISH analysis under DKA exposure

For the control group, miR-184 (Fig. S3A and B) and miR-96 (Fig. S3C and D) showed high expression mainly in the brain, gill, otoliths and lateral line neuromast of 120-hpf zebrafish. DKA-exposed treatments resulted in a significant down-regulation of both miRNAs ($p < 0.05$ or $p < 0.01$) and showed an obvious concentration-dependent relationship. Notably, the significant concentration-dependent down-regulation of miR-184 and miR-96 ($p < 0.05$) was observed in otoliths (Fig. S3E), which suggests that miR-96 and miR-184 might be related to development of the nervous system and sensory organs.

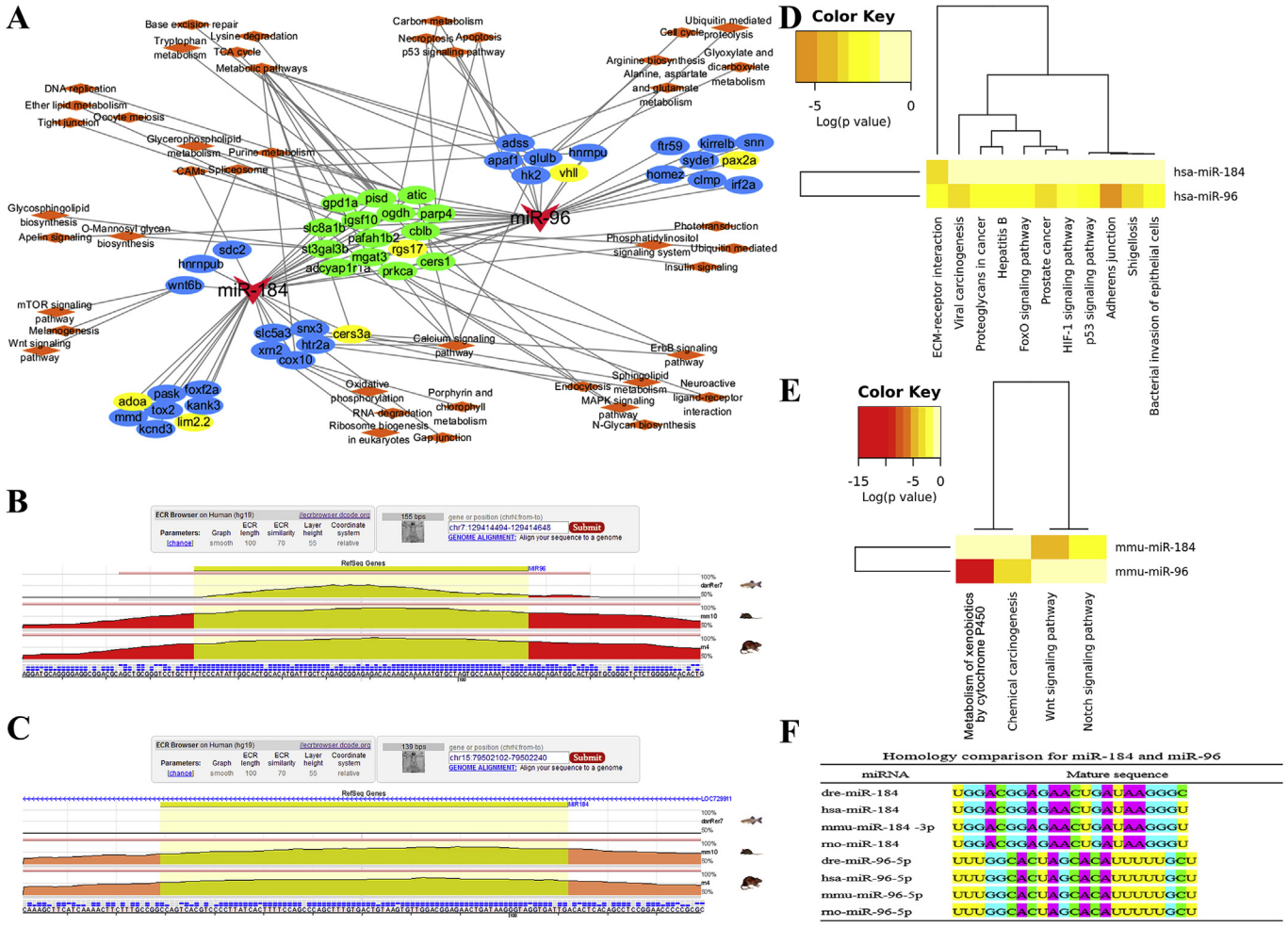

Fig. 1. Regulation network of miR-96 and miR-184, sequence homology and target gene functional pathways. **Notes:** (1) A, regulation network of miR-96 and miR-184, and their related target genes, KEGG pathways; (2) B, sequence homology of miR-96 among humans, rats, mice and zebrafish; (3) C, sequence homology of miR-184 among humans, rats, mice and zebrafish; (4) D, heat map and functional clustering patterns of miR-184 and miR-96 in humans; (5) E, heat map and functional clustering patterns of miR-184 and miR-96 in mice; (6) In Fig. 1A: oval color represents the highly effective binding target genes: blue oval, the highly effective binding targets; green oval, co-regulated by miR-96 and miR-184 targets; yellow oval, selected for verification targets; and orange quadrilateral represents KEGG pathways for targets; (7) Network diagram in Fig. 1A was plotted by Cytoscape (v3.3) software; (8) In heat map of miRNAs *vs.* pathways, miRNAs are clustered together by exhibiting similar pathway targeting patterns, and pathways are clustered together by related miRNAs. (For interpretation of the references to color in this figure legend, the reader is referred to the Web version of this article.)

3.3. Target gene expression of miRNAs by qRT-PCR and W-ISH

Sequences for microRNA mimics and inhibitors of miR-96 and miR-184 were synthesized and injected into zebrafish 1-cell stage embryos (200 ng μL^{-1}, 2 nL per embryo) (Table S3). At 3 dpi (days post-injection), total RNA was isolated and qRT-PCR was used to observe expressions of miR-96 and miR-184. Survival rates in micro-injected mimic and inhibitor treatments were similar to that of the control group (>90%). Both miRNAs were over-expressed following injection of the miR-mimic. In contrast, expressions were significantly inhibited after injection of the miR-inhibitor ($p < 0.05$) (Fig. 2A and B) as compared to negative controls. These results demonstrate that inhibitors and mimics for the two miRNAs responded as expected with respect to function.

Furthermore, target genes with high probability were screened (Table S4), and the expressions of miR-96 and miR-184 were compared by qPCR for 120-hpf larvae between DKA-exposure groups and micro-injected treatment groups (Fig. 2C and D). In DKA-exposure groups, miR-184 or miR-96 showed dose-dependent down-regulation, but *cers3a*, *adoa*, *vhll*, *rgs17* and *syde1* showed a dose-dependent up-regulation. When compared with the control, *sdc2* was up-regulated in the 12.5 mg L^{-1} treatment, but down-regulated in the 25 mg L^{-1} treatment (Fig. 2C). Moreover, both *lim2.2* and *kirrelb* were down-regulated ($p < 0.05$). By comparison, treatments receiving micro-injected inhibitors showed up-regulation of target genes, except for *syde1* (down-regulation) and *cers3a* and *kirrelb* (no significant difference). In contrast, all these genes were significantly down-regulated in micro-injected groups by mimics ($p < 0.05$), suggesting that miRNAs inversely regulate their candidate target genes.

To investigate temporal and spatial distribution and change of target genes during embryonic development, antisense RNA probes for these genes were synthesized by *in vitro* transcription and used for W-ISH analysis. Sequence amplification of target fragments was designed at about 800 bp around 3' UTR (Table S2), products were linked with pEASY-T3 (TransScript) vector, and endonuclease SpeI and NcoI (New England Biolabs, Ipswich, MA, USA) were chosen for plasmid linearization. Plasmid sequences are shown in Fig. S4, and electrophoresis results before and after enzyme digestion are displayed in Fig. S5.

W-ISH results showed that compared with the control group, the temporal and spatial distribution of different genes varied significantly during different stages of embryonic development in DKA-exposure treatments. For miR-184 target genes, the expression of *adoa* was widely present in the brain and spine at 36 hpf, while focused in the brain at 72 hpf. In 120-hpf larvae, *adoa* in the brain was stable with a low expression, which was minimally affected by DKA exposure, and was specifically expressed in the

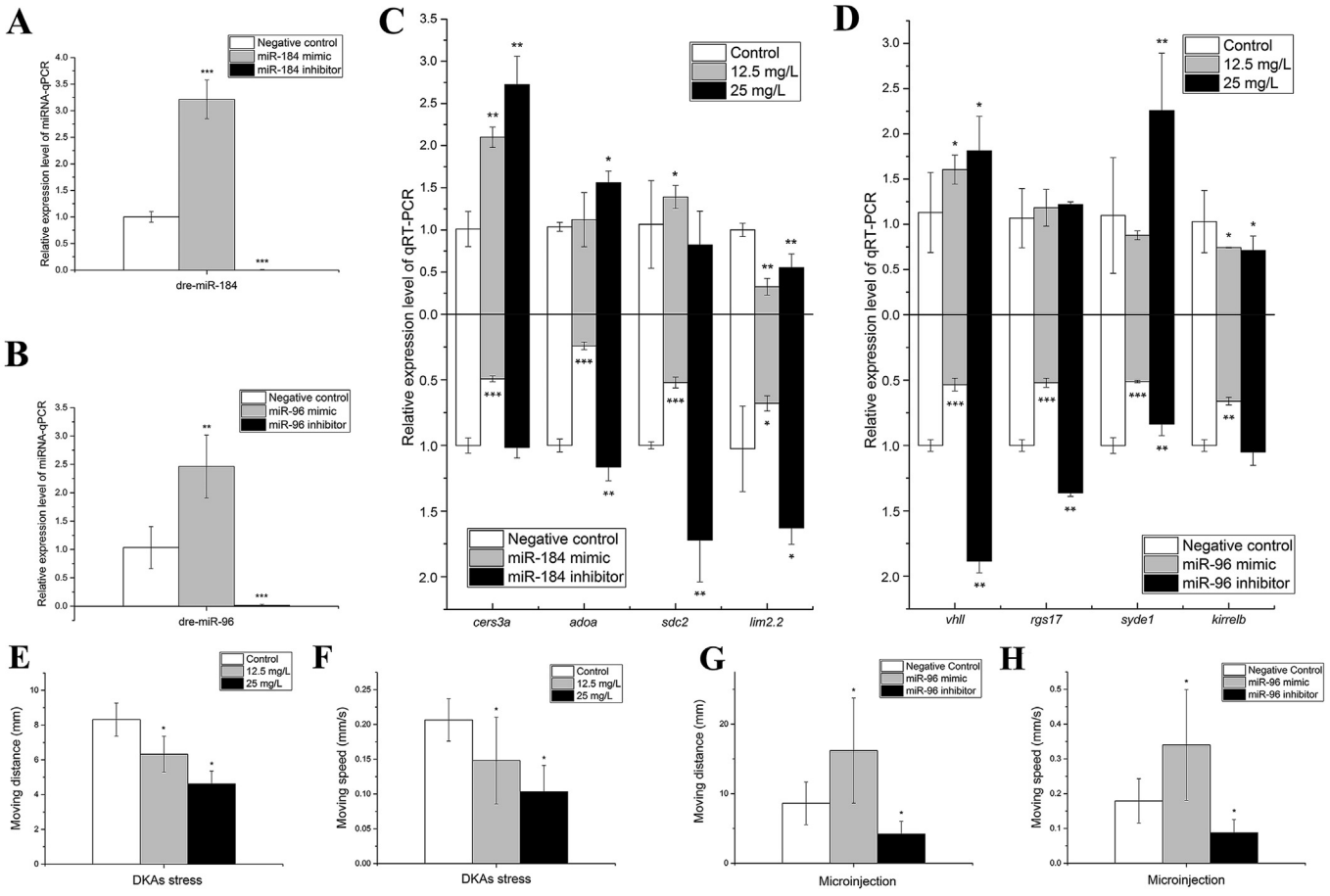

Fig. 2. MiRNA target gene expression after microinjection or DKA exposure by qRT-PCR and response to external auditory stimuli by 120-hpf larvae zebrafish. **Notes:** (1) A, qRT-PCR of miR-184 expression after microinjection in 72-hpf larvae; (2) B, qRT-PCR of miR-96 expression after microinjection in 72-hpf larvae; (3) C, qRT-PCR of miR-184 target gene expression after DKA exposure and microinjection in 120-hpf larvae; (4) D, qRT-PCR of miR-96 target gene expression after DKA exposure and microinjection in 120-hpf larvae; (5) E and F show the response to external auditory stimuli between DKA exposure groups and control group; (6) G and H show the response to external auditory stimuli between microinjection groups and negative control group; (7) *,** and *** in Fig. 2 indicate $p < 0.1$, $p < 0.05$ and $p < 0.01$ respectively, between DKA-exposed treatments and control or microinjection groups and negative control; (8) Dunnett's test statistical analysis.

pancreas, where the hybridization signal was positively correlated with DKA stress (Fig. 3A). Moreover, spatial distribution patterns for the *lim2.2* gene in different embryonic development stages were highly similar to those of *adoa*, but the expression differed with down-regulation in the 12.5 mg L^{-1} DKA treatment and an increase to levels close to the control for the 25 mg L^{-1} DKA treatment (Fig. 3B). Similarly, *cers3a* was mainly expressed in the brain at 36 hpf and was maintained at stable levels without a response to DKA stress until 72 and 120 hpf. Significant differences were found in expression patterns of the larval intestinal system, and the range of expression increased with increasing DKA-exposure concentrations (Fig. 3C).

For miR-96 target genes, *vhll* and *rgs17* were widely expressed in 12-hpf embryos and became concentrated in the head at 48 hpf (Fig. 3D and E). At 120 hpf, *vhll* was specifically expressed in the pancreas, while *rgs17* was primarily expressed in the head. Additionally, the expressions of *vhll* and *rgs17* showed an obvious DKA dose-dependent up-regulation phenomenon.

Two genes, *cers3a* and *rgs17*, were chosen as representative target genes for miR-184 and miR-96, respectively, and their expression patterns were investigated in a manual-intervention miRNA expression model by W-ISH using 72-hpf embryos. W-ISH results showed that the abnormal expression of miR-96 had little effect on expression of *rgs17* in 72-hpf embryos (Fig. 3G), but significant differential expression was observed in the intestinal system whether miR-184 was over-expressed or knocked down (Fig. 3F).

3.4. Behavioral analysis and otic vesicle development

Stress response of larvae to an external acoustic stimulus was used as a criterion for normal development of hearing, and the average speed and swim distance within 15 s after sound stimulation were adopted as two hearing response metrics. After continuous DKA exposure to 120-hpf larval zebrafish, the two response metrics decreased in the 12.5 and 25 mg L^{-1} DKA treatments with a dose-dependent effect, suggesting decreased sensitivity to acoustic stimulation (Fig. 6A and B). Similarly, when compared with the control group, knock-down of miR-96 led to insensitivity to sound stimuli in 120-hpf zebrafish larvae while over-expression of miR-96 resulted in larval overreaction (Fig. 2G and H). These results suggest down-regulation of miR-96 induced by DKA exposure led to similar effects on hearing as those caused by miR-96 knock-down.

Transgene zebrafish (Tg, hue:mcherry) were used for morphological observation of otic vesicle development. Red fluorescence was marked in the saccule and utricle, and the development process was traced by means of temporal and spatial changes in the red fluorescence. Compared to the control group, the development of

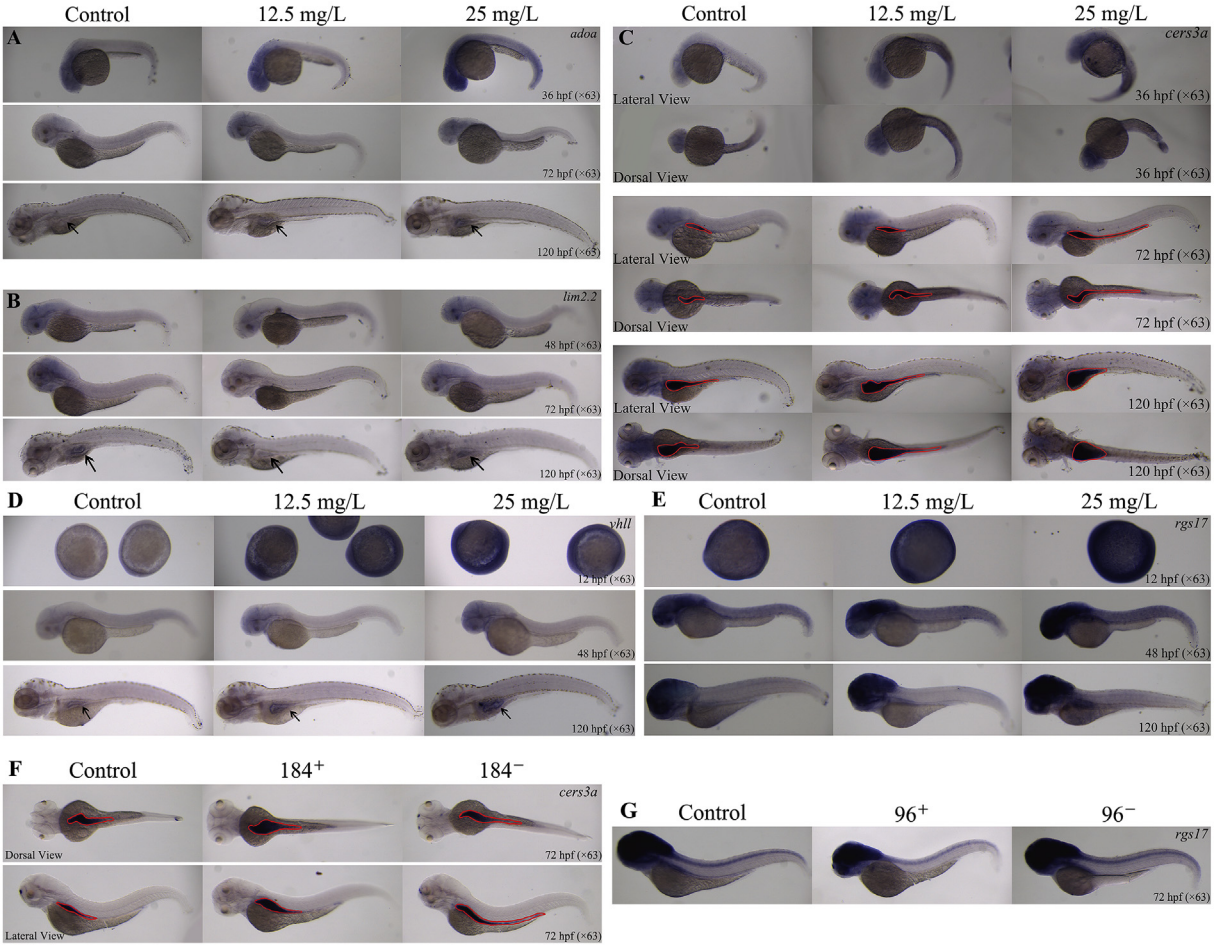

Fig. 3. W-ISH results of miRNA target gene expression after DKA exposure and microinjection. **Notes:** (1) W-ISH of A, *adoa*, B, *lim2.2*, and C, *cers3a*, D, *vhll* and E, *rgs17*expressions during embryo development in control and treatment groups; (2) F, W-ISH of *cers3a* expression in 72-hpf larvae for control and intervention miR-184 expression groups; (3) G, W-ISH of *rgs17* expression in 72-hpf larvae for control and intervention miR-96 expression groups; (4) Arrows in Fig. 3A, B and D indicate the pancreas; (5) Red lines in Fig. 3C and F indicate the intestines. (For interpretation of the references to color in this figure legend, the reader is referred to the Web version of this article.)

otolith was delayed in DKA treatments, which showed unclear boundaries and vacuolization at about 72 hpf. Further, utricular enlargement and decreased saccular volume were observed in development of 96-hpf or older larval otoliths (Fig. S3F). This dose-dependent response implies structural abnormality in the otic vesicle due to DKA exposure.

3.5. Marker gene expression of otoliths by W-ISH

The *pax2a* gene is one of the target genes for miR-96 and is a special marker gene for brain and otic vesicle development. W-ISH was used to trace changes of *pax2a* expression during embryonic development following exposure to DKAs. As shown in Fig. 4A and B, expression of *pax2a* is involved in the origin and development of eyes, mesencephalon and rhombencephalon. For 36-hpf embryos, vesicula optica expression gradually focused on the optic nerve, and also began to appear in the otic vesicle site (Fig. 4C). For 48-hpf or older embryos, stable expression in optic tract, diencephalon, mesencephalon and otic vesicle sites was particularly evident with an increasing dose-dependent effect (Fig. 4D–G).

When expression of miR-96 or miR-184 was manually induced, a significant effect on early embryonic development was observed (Fig. 5A). At the embryonic-larval stages of 12-hpf (Fig. 5A), 72-hpf (Fig. 5B) and 120-hpf (Fig. 5C), over-expression of miR-96 significantly down-regulated the expression of *pax2a*, while knock-down of miR-96 up-regulated *pax2a*. This phenomenon was particularly prominent in the otic vesicle site. In contrast, knock-down of miR-184 caused down-regulation of *pax2a,* while over-expression of miR-184 resulted in up-regulation of *pax2a* in 12-hpf embryos (Fig. 5A). Due to the contrasting effects of the two miRNAs (positive effect for miR-184 and negative effect for miR-96), their combined effects were not pronounced in the course of zebrafish development (Fig. 5B). If the expression of miR-96 and miR-184 changed simultaneously (i.e., one over-expressed and the other knocked-down), a synergistic effect on *pax2a* expression in 12-hpf embryos was noticed (Fig. 5A), but no significant difference was observed in 72-hpf larvae (Fig. 5B).

3.6. Effects of induced miR-96 and miR-184 expression on otoliths development

Compared to the control group, the knock-down of miR-96 exhibited hypoplasia of otoliths in zebrafish embryos, mainly manifested by the reduction of saccule and utricle, which had the same phenotype of otic vesicle as the DKA-exposure treatments. Most larvae produced an extra heteroplasia otolith when miR-96 was over-expressed, demonstrating the overgrowth of the otic vesicle. Additionally, the abnormal expression of miR-96 caused a significant retardation in development of tectum and corpus cerebelli in 24-hpf embryos, but had little influence on ventricle volume in 48-hpf embryos (Fig. 6A) (Eames et al., 2013; Glickman et al., 2003; Kimmel et al., 2010).

Manual intervention of miR-184 expression mainly led to abnormal development in the brain. Accelerated tectum development and cerebellar overgrowth were observed if miR-184 was over-expressed in 24-hpf embryos. Conversely, delayed differentiation of brain and eye was observed if miR-184 was knocked down. For 48-hpf embryos with over-expression of miR-184, the curve of the brain ventricle significantly bulged compared to the control group, suggesting an increase in volume of ventricles. However in the miR-184 knock-down group, the brain ventricle remained smooth and displayed no bulge in the transition to the cerebellum and finally to the spinal cord, suggesting that the volume of brain ventricle was reduced. No obvious change in the utricle was observed if miR-184 was over-expressed, but knock-down of miR-184 led to splitting of the utricle, implying that miR-184 may prevent the over-differentiation of the utricle (Fig. 6B).

Knock down of one miRNA and over-expression of the other miRNA resulted in little influence on morphological development of the otic vesicle. However, simultaneous knock down of miR-96 and miR-184 prominently affected zebrafish normal development. Similarly, over-expression of both miRNAs resulted in three otolith malformations, including an extra unusual otolith nearby the utricle. Abnormal development of the brain was observed for all treatments in 24-hpf embryos (Fig. 6C). At 12-hpf in DKAs-exposed

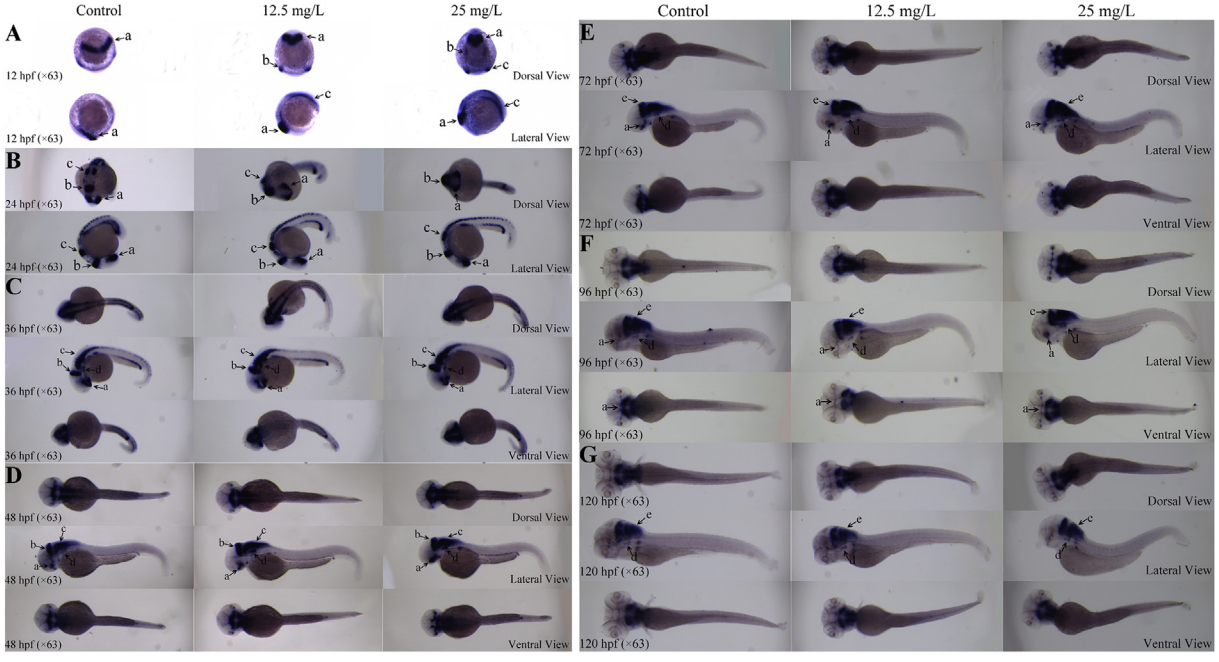

Fig. 4. W-ISH results of *pax2a* expression after DKA exposure. **Notes:** (1) A-G, W-ISH of *pax2a* expression during 12–120 hpf in control and treatment groups; (2) "a arrow" indicates the eyes; (3) "b arrow" indicates the mesencephalon; (4) "c arrow" indicates the rhombencephalon; (5) "d arrow" indicates the otic vesicle; (6) "e arrow" indicates the brain.

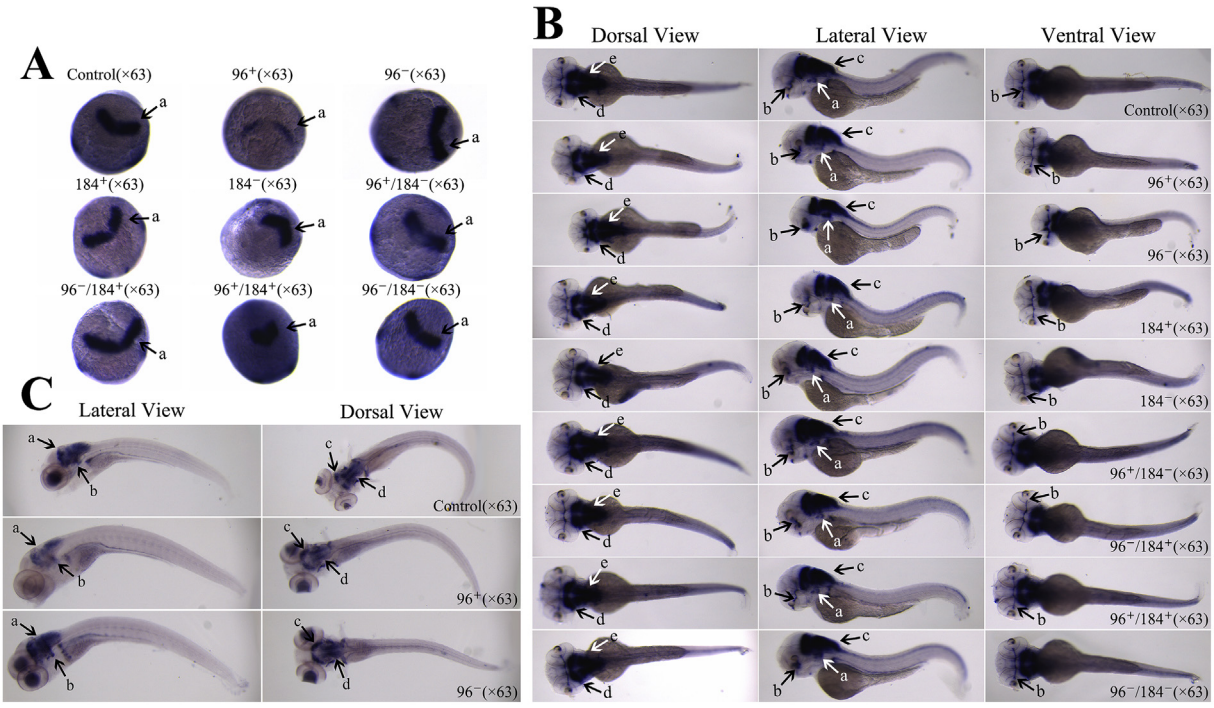

Fig. 5. W-ISH results of *pax2a* expression after induced expression of miR-96 or miR-184. **Notes:** (1) W-ISH of *pax2a* expression at 12 hpf (Fig. 5A), 72 hpf (Fig. 5B) and 120 hpf (Fig. 5C) in control and treatment groups; (2) "a arrow" in Fig. 5A indicates eye primordia; (3) "a arrow" in Fig. 5B indicates theotic vesicle; "b arrow" indicates optic nerve; "c arrow" indicates themesencephalon and rhombencephalon; (4) "a arrow" in Fig. 5C indicates brain; "b arrow" indicates otic vesicle; "c arrow" indicates mesencephalon; "d arrow" indicates rhombencephalon.

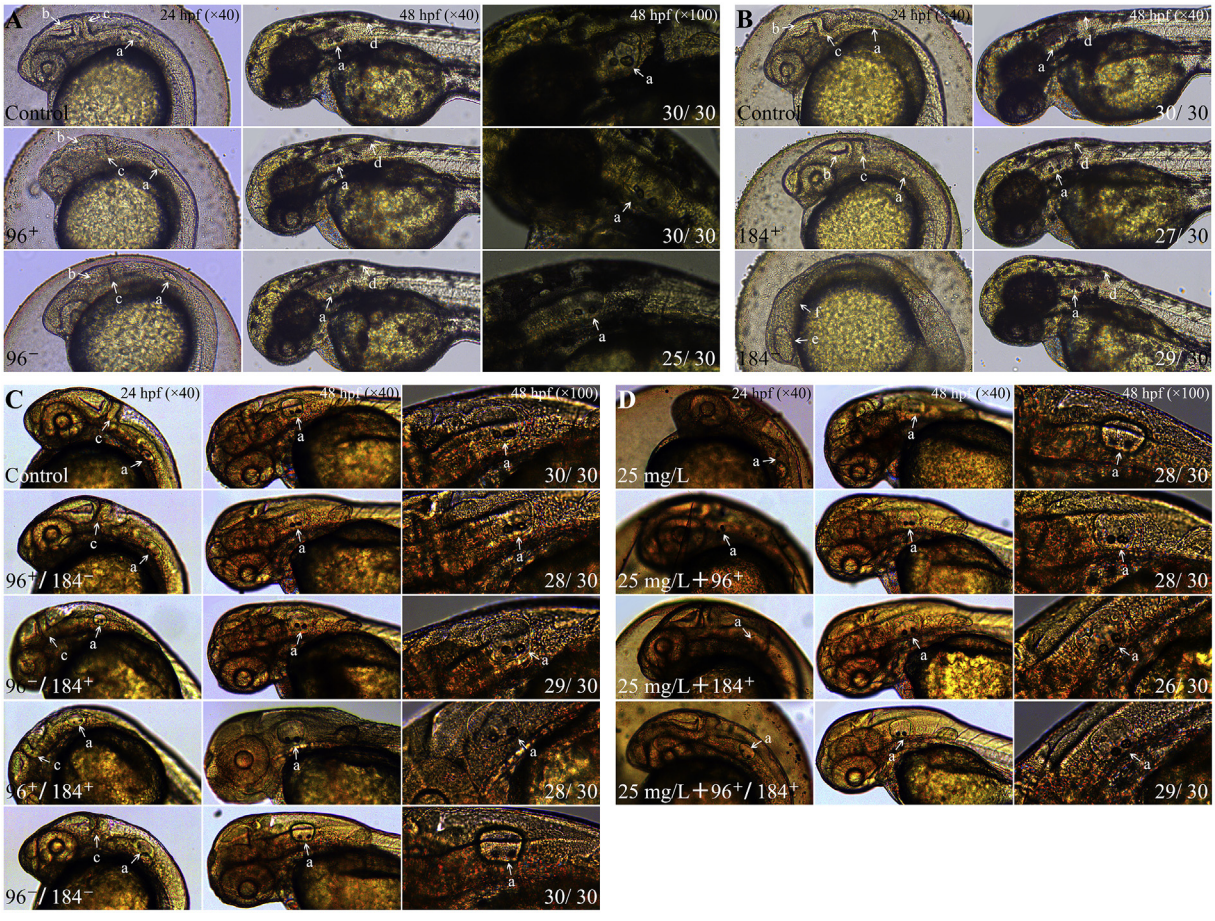

Fig. 6. Morphological observation of zebrafish embryos after knockdown or over expression of miR-96 and miR-184. **Notes:** (1) "a arrow" shows otic vesicle; (2) "b arrow" shows tectum; (3) "c arrow" shows corpus cerebelli; (4) "d arrow" shows ventricle; (5) "e arrow" shows vesicula optica; (6) "f arrow" shows undifferentiated encephalic region.

embryos, injection of miR-96, miR-184 or both miRNA mimics to the yolk sac resulted in marked improvement of the otic vesicle phenotype when observed at 48 hpf (Fig. 6D).

Hair cells are sensory epithelial cells, which are sensitive to sound waves, and function to convert external acoustic signals into neural electrical stimulation in the brain. The number of hair cells in the ear and the maintenance of their normal function are important factors for good hearing (Seymour et al., 2015; Walters et al., 2014). Hair cell staining showed that expression of miR-96 significantly affected the number of hair cells, but this was not the case for expression of miR-184. This phenomenon was similarly observed when the expressions of miR-96 and miR-184 were induced together. No matter how miR-184 was expressed, the number of hair cells was only affected by miR-96 expression (Fig. 7A). Moreover, only the miR-96 mimic-injected treatments restored the number of hair cells after DKA exposure. In contrast, no significant changes were observed in the number of hair cells in miR-184 mimic-injected treatments (Fig. 7B).

AO staining was used for rapid detection of apoptosis in 120-hpf larvae. The over-expressed miR-96 treatment was similar to the control group, showing almost no occurrence of apoptotic phenomenon. The apoptotic signal was detected in gills of miR-96 knocked down treatments, but was not found in the otoliths. When compared to the other two treatments, the contour of otolith was prominently observed in miR-96 over-expressed treatments, which showed a clear fluorescence signal (Fig. 7C). These results suggest that over-expression of miR-96 led to higher otolith cell density than the other two treatments.

4. Discussion

Previous reports in humans and mice revealed that miR-96 and miR-184 were mainly concerned with cell-cycle regulation, and cardiovascular, nervous, digestive and immune system diseases (Table S4) (Malmevik et al., 2016; Wienholds et al., 2005a. Based on high throughput RNA deep sequencing, we found significant miRNA differential expression and a series of physiological changes in tissues and organs after long-term DKA exposure in 2-hpf to 90-dpf zebrafish, especially related to the nervous system (Li et al., 2016b). Of the differentially expressed miRNAs, miR-184 is one of the most typical miRNAs, but few data are available on its functions in zebrafish, although a few studies ascribe an important role in nervous system development of humans and mice (Liang et al., 2017; McKiernan et al., 2012). Additionally, miR-96 was reported as a miR-183 family member whose functions were related to inner ear development and hearing loss (Gu et al., 2013; Kuhn et al., 2011; Lewis et al., 2016). In this study, W-ISH analysis indicated that the expression patterns of miR-96 were very similar to those of miR-184 after DKA exposure (Fig. S3A-D). Informed by the above results, we intensively studied the functional relevance of miR-96 and miR-184 in zebrafish.

The sequence homology of miR-96 and miR-184 among zebrafish, humans, rats and mice (Fig. 1B, C and F) displayed a high degree of homology among species implying their functional conservation. Bioinformatics analyses indicated that miR-96 and miR-184 co-regulated a large number of downstream genes (Fig. 1A) whose functions were enriched in many common signaling pathways (Fig. 1D and E), suggesting their functional

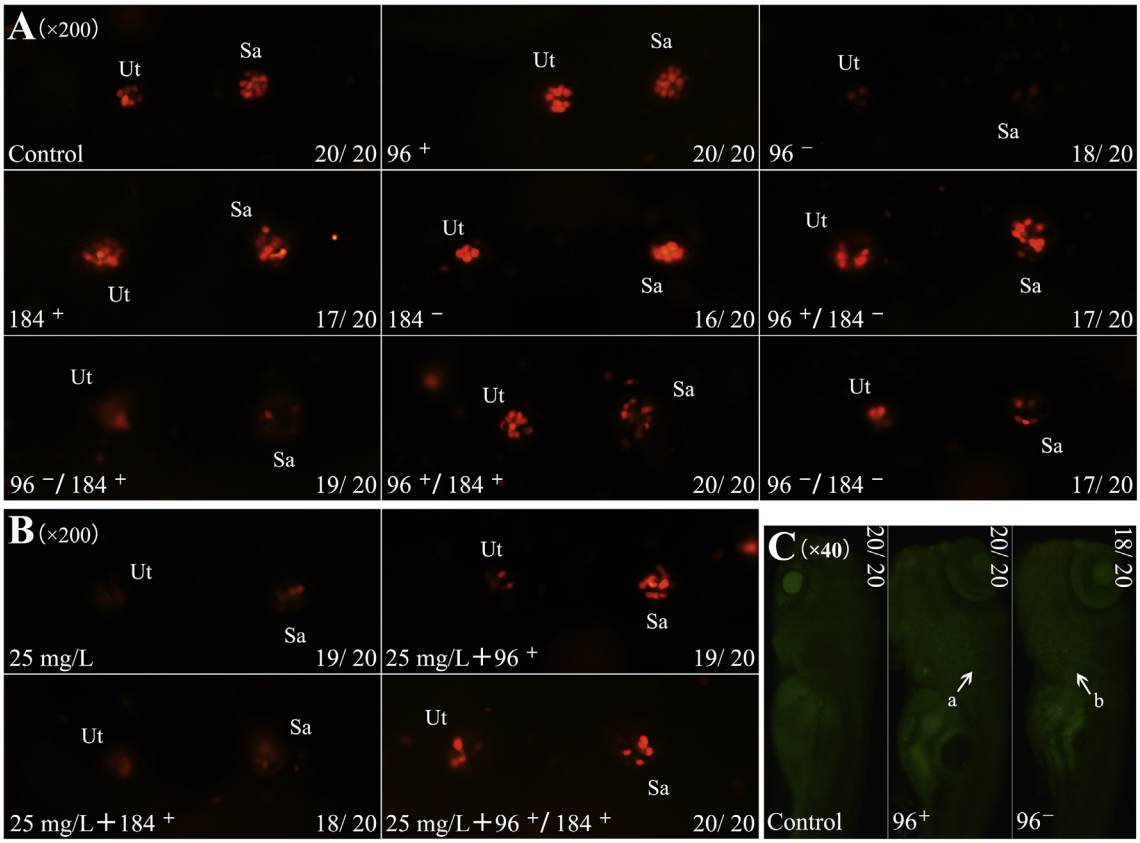

Fig. 7. Hair cell staining and AO staining results. **Notes:** (1) Fig. 7A shows hair cell staining after manual intervention and expression of miR-96 or miR-184; (2) Fig. 7B shows hair cell staining after DKA exposure and up-regulated expression of miR-96 or miR-184; (3) Fig. 7C shows AO staining after over expression or inhibition of miR-96; (4) Abbreviations in Fig. 7A and B: Ut, utricular; Sa, saccular; (5) "a arrow" shows apoptotic signal in Fig. 7C; (6) "b arrow" shows otolith in Fig. 7C.

relevance. Some high binding potential target genes of miR-96 and miR-184 were screened out and their expression patterns determined by qRT-PCR (Fig. 2C and D) and W-ISH (Fig. 3). After DKA exposure, expressions for miR-96 and miR-184 were down-regulated (Fig. S3A-D), which was concomitant with corresponding changes in their downstream target genes. Although the negative regulation between miRNA and its target genes was expected for these changes (Thomson et al., 2011), some were not consistent with theoretical expectations (e.g. *lim2.2*). However, after manual intervention of miR-96 or miR-184 expression, most of these genes were down-regulated after over-expression of miRNA and up-regulated after known-down of miRNA (Fig. 2A and B). These differences may result from genes being regulated by multiple miRNAs or an individual miRNA regulating multiple target genes, forming a complex regulatory network between miRNAs and their target genes (Li et al., 2016b; Nogales-Cadenas et al., 2016; Sun et al., 2017). According to the previous studies, these predicted target genes showed less direct relevance to the hair cell development or hearing loss. But some of them were correlated to the vascular and neuron development, and may indirectly influence normal development of the otoliths. For instance, *sdc2* was an important factor during zebrafish vascular and brain development, while *lim2.2* was essential for the retina (Chen et al., 2004; Hofmeister et al., 2013; Vihtelic et al., 2005).

Abnormal development of otoliths in zebrafish embryos (Fig. S3F) and a decreased sensitivity to acoustic reflex (Fig. 2E and F) were observed following DKA exposure, which suggests hearing impairment. Decreased acoustic sensitivity occurred in the miR-96-knocked down group while increased sensitivity was found in the miR-96 over-expression group in zebrafish larvae (Fig. 2G and H), consistent with previous reports in mice and human (Lewis et al., 2016; Li et al., 2010). Temporal and spatial expression of the neural marker gene *pax2a*, a miR-96 target gene and one of the hearing-associated genes (Hu et al., 2013), was detected by W-ISH to track development of the sensory system (Gu et al., 2013; Padanad et al., 2011). Expression changes for *pax2a* were found in the otic vesicle, optic tract, optic tectum and cerebellum (Fig. 4). A prominent up-regulation of *pax2a* was observed in the otic vesicle, suggesting disorder of the nerve sensing system after DKA exposure (Duncan et al., 2015; Ullmann et al., 2010). Similar expression changes in the otic vesicle were observed in miR-96 knocked down or over-expression groups (Fig. 5). However, expression of *pax2a* appeared to be insensitive to changes in miR-184 expression. That is to say, no matter how miR-184 was expressed, the expression of *pax2a* was mainly regulated by miR-96, showing a negative dependence (Fig. 5).

Morphological observations showed that both up-regulation and down-regulation of miR-96 severely retarded brain differentiation in 24-hpf embryos. It was almost impossible to distinguish between tectum and cerebellum with distinctive signs of brain differentiation (Kimmel et al., 1995). As compared with the control group, DKA exposure did not cause any differences in brain phenotype in 48-hpf embryos (Fig. 6A). The over-expression of miR-184 significantly increased brain development, but knock-down inhibited differentiation of the brain and development of eyes in 24-hpf embryos (Fig. 6B). These results suggest that miR-96 and miR-184 have some functional relevance to early stage brain development. The abnormal expression of miR-96 significantly affected the development of otoliths (Fig. 6A), which was consistent with our previous findings (Li et al., 2016b). Notably, knock-down of miR-96 and over-expression of miR-184 (or the knock-down of miR-184 and over-expression of miR-96) led to no obvious abnormalities of otic vesicle morphology (Fig. 6C).

After DKA exposure, micro-injection of miR-96 and/or miR-184 mimics into zebrafish embryos markedly improved the otoliths phenotype (Fig. 6D). By means of hair cell staining, we observed that as compared with miR-96, the abnormal expression of miR-184 showed no significant effect on hair cells. No matter how miR-184 was expressed, the number of hair cells only increased when miR-96 was over-expressed, and decreased when miR-96 was inhibited (Fig. 7A). Moreover, hair cell staining demonstrated that after DKA exposure, only the up-regulation of miR-96 could recover the number of hair cells; changes in miR-184 expression had no effect (Fig. 7B). These observations imply that miR-96 plays an important role in development of the otic vesicle and formation of hearing, and that miR-184 is only involved in construction of the otic vesicle during zebrafish embryonic development.

Acknowledgements

This work is jointly supported by the National Natural Science Foundation of China (31770552 and 21876125), the Natural Science Foundation of Zhejiang Province (LY17H260004 and LY17B070005), and the Nucleic Acids Based Molecular Diagnostics Innovative Discipline, Health and Family Planning Commission of Zhejiang Province.

Appendix A. Supplementary data

Supplementary data to this article can be found online at https://doi.org/10.1016/j.chemosphere.2018.09.118.

References

Brain, R.A., Wilson, C.J., Johnson, D.J., Sanderson, H., Bestari, K.J., Hanson, M.L., Sibley, P.K., Solomon, K.R., 2005. Effects of a mixture of tetracyclines to *Lemna gibba* and *Myriophyllum sibiricum* evaluated in aquatic microcosms. Environ. Pollut. 138, 425–442. https://doi.org/10.1016/j.envpol.2005.04.021.

Chen, E., Hermanson, S., Ekker, S.C., 2004. Syndecan-2 is essential for angiogenic sprouting during zebrafish development. Blood 103, 1710–1719. https://doi.org/10.1182/blood-2003-06-1783.

Chotmongkol, V., Sawanyawisuth, K., Yimtae, K., Chantarojanasiri, T., Chotmongkol, R., 2012. Doxycycline treatment of otosyphilis with hearing loss. Sex. Transm. Infect. 88, 177–178. https://doi.org/10.1136/sextrans-2011-050201.

Corbacella, E., Lanzoni, I., Ding, D., Previati, M., Salvi, R., 2004. Minocycline attenuates gentamicin induced hair cell loss in neonatal cochlear cultures. Hear. Res. 197, 11–18. https://doi.org/10.1016/j.heares.2004.03.012.

Ding, G., Zhang, J., Chen, Y., Wang, L., Wang, M., Xiong, D., Sun, Y., 2013. Combined effects of PFOS and PFOA on zebrafish (Danio rerio) embryos. Arch. Environ. Contam. Toxicol. 64, 668–675. https://doi.org/10.1007/s00244-012-9864-2.

Duncan, R.N., Panahi, S., Piotrowski, T., Dorsky, R.I., 2015. Identification of Wnt genes expressed in neural progenitor zones during zebrafish brain development. PLoS One 10, e0145810. https://doi.org/10.1371/journal.pone.0145810.

Eames, B.F., DeLaurier, A., Ullmann, B., Huycke, T.R., Nichols, J.T., Dowd, J., McFadden, M., Sasaki, M.M., Kimmel, C.B., 2013. FishFace: interactive atlas of zebrafish craniofacial development at cellular resolution. BMC Dev. Biol. 28, 13–23. https://doi.org/10.1186/1471-213X-13-23.

Etminan, M., Westerberg, B.D., Kozak, F.K., Guo, M.Y., Carleton, B.C., 2017. Risk of sensorineural hearing loss with macrolide antibiotics: a nested case-control study. Laryngoscope 127, 229–232. https://doi.org/10.1002/lary.26190.

Glickman, N.S., Kimmel, C.B., Jones, M.A., Adams, R.J., 2003. Shaping the zebrafish notochord. Development 130, 873–887. https://doi.org/10.1242/dev.00314.

Gu, C., Li, X., Tan, Q., Wang, Z., Chen, L., Liu, Y., 2013. MiR-183 family regulates chloride intracellular channel 5 expression in inner ear hair cells. Toxicol. Vitro 27, 486–491. https://doi.org/10.1016/j.tiv.2012.07.008.

Hofmeister, W., Devine, C.A., Key, B., 2013. Distinct expression patterns of syndecans in the embryonic zebrafish brain. Gene. Expr. Patterns 13, 126–132. https://doi.org/10.1016/j.gep.2013.02.002.

Hu, Z.Y., Zhang, Q.Y., Qin, W., Tong, J.W., Zhao, Q., Han, Y., Meng, J., Zhang, J.P., 2013. Gene miles-apart is required for formation of otic vesicle and hair cells in zebrafish. Cell Death Dis. 4, e900 https://doi.org/10.1038/cddis.2013.432.

Huang, da W., Sherman, B.T., Lempicki, R.A., 2009. Bioinformatics enrichment tools: paths toward the comprehensive functional analysis of large gene lists. Nucleic Acids Res. 37, 1–13. https://doi.org/10.1093/nar/gkn923.

Kaur, S., Lotsari-Salomaa, J.E., Seppänen-Kaijansinkko, R., Peltomäki, P., 2016. MicroRNA methylation in colorectal cancer. Adv. Exp. Med. Biol. 937, 109–122. https://doi.org/10.1007/978-3-319-42059-2_6.

Kimmel, C.B., Ballard, W.W., Kimmel, S.R., Ullmann, B., Schilling, T.F., 1995. Stages of embryonic development of the zebrafish. Dev. Dynam. 203, 253–310. https://doi.org/10.1002/aja.1002030302.

Kimmel, C.B., DeLaurier, A., Ullmann, B., Dowd, J., McFadden, M., 2010. Modes of

developmental outgrowth and shaping of a craniofacial bone in zebrafish. PLoS One 5, e9475. https://doi.org/10.1371/journal.pone.0009475.
Kuhn, S., Johnson, S.L., Furness, D.N., Chen, J., Ingham, N., Hilton, J.M., Steffes, G., Lewis, M.A., Zampini, V., Hackney, C.M., Masetto, S., Holley, M.C., Steel, K.P., Marcotti, W., 2011. miR-96 regulates the progression of differentiation in mammalian cochlear inner and outer hair cells. Proc. Nat. Acad. Sci. 108, 2355–2360. https://doi.org/10.1073/pnas.1016646108.
Lewis, M.A., Buniello, A., Hilton, J.M., Zhu, F., Zhang, W.I., Evans, S., van Dongen, S., Enright, A.J., Steel, K.P., 2016. Exploring regulatory networks of miR-96 in the developing inner ear. Sci. Rep. 6, 23363. https://doi.org/10.1038/srep23363.
Liang, X.G., Meng, W.T., Hu, L.J., Li, L., Xing, H., Xie, G., Wang, A.Q., Jia, Y.Q., 2017. MicroRNA-184 modulates human central nervous system lymphoma cells growth and invasion by targeting iASPP. J. Cell. Biochem. 118, 2645–2653. https://doi.org/10.1002/jcb.25856.
Li, F., Wang, H., Liu, J., Lin, J., Zeng, A., Ai, W., Wang, X., Dahlgren, R.A., Wang, H., 2016a. Immunotoxicity of β-diketone antibiotic mixtures to zebrafish (Danio rerio) by transcriptome analysis. PLoS One 11, e0152530. https://doi.org/10.1371/journal.pone.0152530.
Li, H., Kloosterman, W., Fekete, D.M., 2010. MicroRNA-183 family members regulate sensorineural fates in the inner ear. J. Neurosci. 30, 3254–3263. https://doi.org/10.1523/JNEUROSCI.4948-09.2010.
Li, J., Liu, J., Zhang, Y., Wang, X., Li, W., Zhang, H., Wang, H., 2016b. Screening on the differentially expressed miRNAs in zebrafish (Danio rerio) exposed to trace β-diketone antibiotics and their related functions. Aquat. Toxicol. 178, 27–38. https://doi.org/10.1016/j.aquatox.2016.07.009.
Livak, K.J., Schmittgen, T.D., 2001. Analysis of relative gene expression data using real-time quantitative PCR and the 2(-Delta Delta C(T)) method. Methods 25, 402–408. https://doi.org/10.1006/meth.2001.1262.
Malmevik, J., Petri, R., Knauff, P., Brattås, P.L., Åkerblom, M., Jakobsson, J., 2016. Distinct cognitive effects and underlying transcriptome changes upon inhibition of individual miRNAs in hippocampal neurons. Sci. Rep. 6, 19879. https://doi.org/10.1038/srep19879.
McKiernan, R.C., Jimenez-Mateos, E.M., Sano, T., Bray, I., Stallings, R.L., Simon, R.P., Henshall, D.C., 2012. Expression profiling the microRNA response to epileptic preconditioning identifies miR-184 as a modulator of seizure-induced neuronal death. Exp. Neurol. 237, 346–354. https://doi.org/10.1016/j.expneurol.2012.06.029.
Melvin, S.D., Cameron, M.C., Lanctot, C.M., 2014. Individual and mixture toxicity of pharmaceuticals naproxen, carbamazepine, and sulfamethoxazole to Australian striped marsh frog tadpoles (Limnodynastes peronii). J. Toxicol. Environ. Health 77, 337–345. https://doi.org/10.1080/15287394.2013.865107.
Mulgaonkar, A., Venitz, J., Sweet, D.H., 2012. Fluoroquinolone disposition: identification of the contribution of renal secretory and reabsorptive drug transporters. Expert Opin. Drug Met 8, 553–559. https://doi.org/10.1517/17425255.2012.674512.
Nogales-Cadenas, R., Cai, Y., Lin, J.R., 2016. MicroRNA expression and gene regulation drive breast cancer progression and metastasis in PyMT mice. Breast Canc. Res. 18, 75. https://doi.org/10.1186/s13058-016-0735-z.
Owens, K.N., Coffin, A.B., Hong, L.S., O'Connell Bennett, K., Rubel, E.W., Raible, D.W., 2009. Response of mechanosensory hair cells of the zebrafish lateral line to aminoglycosides reveals distinct cell death pathways. Hear. Res. 253, 32–41. https://doi.org/10.1016/j.heares.2009.03.001.
Padanad, M.S., Riley, B.B., 2011. Pax2/8 proteins coordinate sequential induction of otic and epibranchial placodes through differential regulation of foxi1, sox3 and fgf24. Dev. Biol. 351, 90–98. https://doi.org/10.1016/j.ydbio.2010.12.036.
Qu, S., Wang, X., Tong, C., Wu, J., 2010. Metal ion mediated molecularly imprinted polymer for selective capturing antibiotics containing beta-diketone structure. J. Chromatogr. A 1217, 8205–8211. https://doi.org/10.1016/j.chroma.2010.10.097.
Sarmah, A.K., Meyer, M.T., Boxall, A.B., 2006. A global perspective on the use, sales, exposure pathways, occurrence, fate and effects of veterinary antibiotics (VAs) in the environment. Chemosphere 65, 725–759. https://doi.org/10.1016/j.chemosphere.2006.03.026.
Samarei, R., 2014. Comparison of local and systemic ciprofloxacin ototoxicity in the treatment of chronic media otitis. Global J. Health Sci. 18, 144–149. https://doi.org/10.5539/gjhs.v6n7p144.
Sun, L., Sun, J., Li, X., Zhang, L., Yang, H., Wang, Q., 2017. Understanding regulation of microRNAs on intestine regeneration in the sea cucumber Apostichopus japonicus using high-throughput sequencing. Comp. Biochem. Physiol. Genom. Proteonomics 22, 1–9. https://doi.org/10.1016/j.cbd.2017.01.001.
Seymour, M.L., Pereira, F.A., 2015. Survival of auditory hair cells. Cell Tissue Res. 361, 59–63. https://doi.org/10.1007/s00441-015-2152-5.
Soldà, G., Robusto, M., Primignani, P., Castorina, P., Benzoni, E., Cesarani, A., Ambrosetti, U., Asselta, R., Duga, S., 2012. A novel mutation within the MIR96 gene causes non-syndromic inherited hearing loss in an Italian family by altering pre-miRNA processing. Hum. Mol. Genet. 21, 577–585. https://doi.org/10.1093/hmg/ddr493.
Thisse, C., Thisse, B., 2008. High-resolution in situ hybridization to whole-mount zebrafish embryos. Nat. Protoc. 3, 59–69. https://doi.org/10.1038/nprot.2007.514.
Thomson, D.W., Bracken, C.P., Goodall, G.J., 2011. Experimental strategies for microRNA target identification. Nucleic Acids Res. 39, 6845–6853. https://doi.org/10.1093/nar/gkr330.
Ullmann, J.F., Cowin, G., Kurniawan, N.D., Collin, S.P., 2010. A three-dimensional digital atlas of the zebrafish brain. Neuroimage 51, 76–82. https://doi.org/10.1016/j.neuroimage.2010.01.086.
Vlachos, I.S., Zagganas, K., Paraskevopoulou, M.D., Georgakilas, G., Karagkouni, D., Vergoulis, T., Dalamagas, T., Hatzigeorgiou, A.G., 2015. DIANA-miRPath v3.0: deciphering microRNA function with experimental support. Nucleic Acids Res. 43, W460–W466. https://doi.org/10.1093/nar/gkv403.
Vihtelic, T.S., Fadool, J.M., Gao, J., Thornton, K.A., Hyde, D.R., Wistow, G., 2005. Expressed sequence tag analysis of zebrafish eye tissues for NEIBank. Mol. Vis. 11, 1083–1100.
Walters, B.J., Liu, Z., Crabtree, M., Coak, E., Cox, B.C., Zuo, J., 2014. Auditory hair cell-specific deletion of p27Kip1 in postnatal mice promotes cell-autonomous generation of new hair cells and normal hearing. J. Neurosci. 34, 15751–15763. https://doi.org/10.1523/JNEUROSCI.3200-14.2014.
Wang, H., Che, B., Duan, A., Mao, J., Dahlgren, R.A., Zhang, M., Zhang, H., Zeng, A., Wang, X., 2014. Toxicity evaluation of β-diketone antibiotics on the development of embryo-larval zebrafish (Danio rerio). Environ. Toxicol. 29, 1134–1146. https://doi.org/10.1002/tox.21843.
Wang, N., Nkejabega, N., Hien, N.N., Huynh, T.T., Silvestre, F., Phuong, N.T., Danyi, S., Widart, J., Douny, C., Scippo, M.L., Kestemont, P., Huong, D.T., 2009. Adverse effects of enrofloxacin when associated with environmental stress in Tra catfish (*Pangasianodon hypophthalmus*). Chemosphere 77, 1577–1584. https://doi.org/10.1016/j.chemosphere.2009.09.038.
Westerfield, M., 1995. The Zebrafish Book: a Guide for the Laboratory Use of Zebrafish (Danio rerio). University of Oregon Press, Eugene, pp. 267–272.
Wienholds, E., Kloosterman, W.P., Miska, E., Alvarez-Saavedra, E., Berezikov, E., de Bruijn, E., Horvitz, H.R., Kauppinen, S., Plasterk, R.H., 2005a. MicroRNA expression in zebrafish embryonic development. Science 309, 310–311. https://doi.org/10.1126/science.1114519.
Wienholds, E., Plasterk, R.H., 2005b. MicroRNA function in animal development. FEBS Lett. 579, 5911–5922. https://doi.org/10.1016/j.febslet.2005.07.070.
Wu, Q., Zhang, J., Koh, W., Yu, Q., Zhu, X., Amsterdam, A., Davis, G.E., Arnaout, M.A., Xiong, J.W., 2015. Talin1 is required for cardiac Z-disk stabilization and endothelial integrity in zebrafish. Faseb. J. 29, 4989–5005. https://doi.org/10.1096/fj.15-273409.
Xu, B., Zhang, Y., Du, X.F., Li, J., Zi, H.X., Bu, J.W., Yan, Y., Han, H., Du, J.L., 2017. Neurons secrete miR-132-containing exosomes to regulate brain vascular integrity. Cell Res. 27, 882–897. https://doi.org/10.1038/cr.2017.62.
Yang, V.K., Loughran, K.A., Meola, D.M., Juhr, C.M., Thane, K.E., Davis, A.M., Hoffman, A.M., 2017. Circulating exosome microRNA associated with heart failure secondary to myxomatous mitral valve disease in a naturally occurring canine model. J. Extracell. Vesicles 6, 1350088. https://doi.org/10.1080/20013078.2017.1350088.
Yin, H.Q., Kim, M., Kim, J.H., Kong, G., Lee, M.O., Kang, K.S., Yoon, B.I., Kim, H.L., Lee, B.H., 2006. Hepatic gene expression profiling and lipid homeostasis in mice exposed to steatogenic drug, tetracycline. Toxicol. Sci. 94, 206–216. https://doi.org/10.1093/toxsci/kfl078.
Yoon, Y., Ryu, J., Oh, J., Choi, B.G., Snyder, S.A., 2010. Occurrence of endocrine disrupting compounds, pharmaceuticals, and personal care products in the Han River (Seoul, South Korea). Sci. Total Environ. 408, 636–643. https://doi.org/10.1016/j.scitotenv.2009.10.049.
Zhao, L., Sun, H., Kong, H., Chen, Z., Chen, B., Zhou, M., 2017. The Lncrna-TUG1/EZH2 axis promotes pancreatic cancer cell proliferation, migration and EMT phenotype formation through sponging Mir-382. Cell. Physiol. Biochem. 42, 2145–2158. https://doi.org/10.1159/000479990.
Zhou, Y., Wang, X., Zhang, J., He, A., Wang, Y.L., Han, K., Su, Y., Yin, J., Lv, X., Hu, H., 2017. Artesunate suppresses the viability and mobility of prostate cancer cells through UCA1, the sponge of miR-184. Oncotarget 8, 18260–18270. https://doi.org/10.18632/oncotarget.15353.